

Delay-induced wave instabilities in single-species reaction-diffusion systemsAndreas Otto,^{*} Jian Wang,[†] and Günter Radons[‡]*Institute of Physics, Chemnitz University of Technology, D-09107 Chemnitz, Germany*

(Received 21 July 2017; published 3 November 2017)

The Turing (wave) instability is only possible in reaction-diffusion systems with more than one (two) components. Motivated by the fact that a time delay increases the dimension of a system, we investigate the presence of diffusion-driven instabilities in single-species reaction-diffusion systems with delay. The stability of arbitrary one-component systems with a single discrete delay, with distributed delay, or with a variable delay is systematically analyzed. We show that a wave instability can appear from an equilibrium of single-species reaction-diffusion systems with fluctuating or distributed delay, which is not possible in similar systems with constant discrete delay or without delay. More precisely, we show by basic analytic arguments and by numerical simulations that fast asymmetric delay fluctuations or asymmetrically distributed delays can lead to wave instabilities in these systems. Examples, for the resulting traveling waves are shown for a Fisher-KPP equation with distributed delay in the reaction term. In addition, we have studied diffusion-induced instabilities from homogeneous periodic orbits in the same systems with variable delay, where the homogeneous periodic orbits are attracting resonant periodic solutions of the system without diffusion, i.e., periodic orbits of the Hutchinson equation with time-varying delay. If diffusion is introduced, standing waves can emerge whose temporal period is equal to the period of the variable delay.

DOI: [10.1103/PhysRevE.96.052202](https://doi.org/10.1103/PhysRevE.96.052202)**I. INTRODUCTION**

In 1952 Turing published a paper which describes a mechanism for pattern formation [1], emphasizing that diffusion can induce an instability of a spatially homogeneous solution. Intuitively, diffusion erases spatial inhomogeneities and stabilizes the homogeneous states. For instance, a drop of ink put into water diffuses through the water, and after a long period of time no color differences will be detected in the water. In contrast, Turing has shown that diffusion can also cause a breaking of the spatial symmetry, which drives the system away from the homogeneous stable state. This type of instability is called Turing instability. At first, Turing patterns were considered as just an isolated phenomenon and a theoretical hypothesis, and the Turing instability has not been considered as the origin of patterns in nature and experiments. Hence, his paper did not attract much attention until Prigogine and Nicolis advanced the dissipative structure theory [2]. Scientists realized that self-organized pattern formation relies on universal mechanisms and Turing's theoretical paper became more relevant. While Turing patterns in the strict sense are constant in time, the time-periodic equivalent of the Turing instability is often called wave instability. The wave instability is characterized by spatially inhomogeneous oscillations that appear from homogeneous states due to the introduction of diffusion [3]. Pattern formation due to diffusion-driven instabilities such as the classical Turing instability or the wave instability is studied, for example, in Refs. [4–6].

On the other hand, time-delay systems are studied in various fields. With the introduction of time delays into dynamical systems, theoretical models become more realistic. Time-delay systems can be found, for example, in optics [7],

engineering [8], control theory [9,10], biology, and physiology [11,12]. The influence of time delays was also studied for spatially extended systems. For instance, there are results for the general stability, and in bifurcation analysis [13–16], the analysis of spatiotemporal structures [17–19], the control of localized structures via time-delay feedback [20], and in the analysis of Turing instabilities in reaction-diffusion systems [21–23].

A well-known example and one of the simplest models of a single-species reaction-diffusion equation is the Fisher-KPP equation. It was introduced in two independent publications in 1937 [24,25]. The equation is used as a spatially extended model for the analysis of population dynamics and has much been used for studying the propagation of front solutions. Diffusion-induced instabilities are not possible for single-species reaction-diffusion systems without delay because at least two species are necessary, as it was shown in the original Turing paper [1]. When a time delay appears, the dimension of the system increases and diffusion-induced instabilities might be possible. Such systems are to some extent related to multiple-component systems with only one diffuser, where diffusion-induced instabilities are possible [26–28]. The existence of Turing-like waves for a single-species delayed reaction-diffusion model on a complex network was already reported in [29], where a constant time delay was introduced in the diffusion along the network. Moreover, spatiotemporal patterns in single-species reaction-diffusion systems with small fluctuating delays in the diffusion term were found in [30].

In this paper we study systematically the existence of diffusion-induced instabilities for general single-species reaction-diffusion systems with a delay in the reaction term,

$$\frac{\partial u(\mathbf{x},t)}{\partial t} = f(u(\mathbf{x},t), u_\tau(\mathbf{x},t)) + D\Delta u(\mathbf{x},t), \quad (1)$$

where the scalar field $u(\mathbf{x},t)$ can be considered as the concentration of some substance in n dimensions, $\mathbf{x} \in \mathbb{R}^n$.

^{*}otto.a@mail.de[†]jianwn@hotmail.com[‡]radons@physik.tu-chemnitz.de

The delay variable $u_\tau(\mathbf{x}, t)$ in the reaction term is given by a superposition of delayed states of the form

$$u_\tau(\mathbf{x}, t) = \int_{\tau_{\min}}^{\tau_{\max}} \rho(t, \tau) u(\mathbf{x}, t - \tau) d\tau, \quad (2)$$

where $\rho(t, \tau) \geq 0$ is the delay distribution with nonzero values between the minimal and the maximal delay τ_{\min} and τ_{\max} , respectively. The delay distribution is normalized to 1, that is, $\int_{\tau_{\min}}^{\tau_{\max}} \rho(t, \tau) d\tau = 1$. Equation (1) with a nondelayed reaction term of the form $f = au(1 - u)$ is equivalent to the above-mentioned Fisher-KPP equation. On the other hand, Eq. (1) with a delay in the reaction term $f = au(1 - u_\tau)$ but without diffusion ($D = 0$) is a generalization of the Hutchinson equation. In particular, this equation with one constant delay τ_0 , i.e., with $\rho(t, \tau) = \delta(\tau - \tau_0)$, where δ denotes the Dirac δ function, was introduced in 1948 by Hutchinson to form a more realistic logistic model for population dynamics [31]. In systems like Eq. (1) the current state u and the delayed state u_τ in the reaction term can play the role of an *activator* and an *inhibitor*, which facilitates and prevents its own reproduction, respectively. In this case the Hutchinson equation can produce oscillatory solutions which are not possible in the classical logistic equation. It is natural to study the interaction between diffusion and delay in these models for population dynamics.

For instance, in population dynamics the delay in Eq. (1) may specify the time to reach sexual maturity of a species, which is typically given by a threshold condition [32]. Under well-controlled laboratory conditions it may be reasonable to assume a unique constant velocity of maturation (development rate) leading to a constant discrete delay. However, in a more realistic scenario the environmental conditions may change, leading to a time-varying development rate and time-varying delays [33, 34]. On the other hand, the development rate and therefore the time delay is, in general, not the same for all individuals of a species, which leads to a distribution of delays. Thus, we consider three different types of delays: (1) a constant discrete delay τ_0 , $\rho(t, \tau) = \delta(\tau - \tau_0)$, (2) a constant distributed delay with more than one discrete delay, $\rho(t, \tau) = \sum_i \delta(\tau - \tau_i)$, or a continuous delay distribution, and (3) a discrete time-varying delay $\tau_0(t) = \tau_0(t + T_p)$ with period T_p , $\rho(t, \tau) = \delta(\tau - \tau_0(t))$.

The paper is organized as follows. The linear stability analysis of Eq. (1) and the numerical methods used are presented in Sec. II. Diffusion-induced instabilities from homogeneous equilibria of the system Eq. (1) with time-invariant delays are systematically studied in Sec. III. The stability of equilibria in the case of a fluctuating time delay is analyzed in Sec. IV, where the limiting cases of slow and fast time variations of the delay are connected to the analytical results for constant delays. In Sec. V diffusion-induced instabilities from stable periodic orbits in the Fisher-KPP equation with delay are discussed, and closing remarks are given in Sec. VI.

II. STABILITY ANALYSIS

In this section the linear stability of Eq. (1) is analyzed for reference solutions $\bar{u}(\mathbf{x}, t)$ of one-component reaction-diffusion systems with delay by determining the asymptotic behavior of small perturbations $\xi(\mathbf{x}, t) = u(\mathbf{x}, t) - \bar{u}(\mathbf{x}, t)$. The

linearized dynamics can be described by

$$\frac{\partial \xi(\mathbf{x}, t)}{\partial t} = (\alpha(\mathbf{x}, t) + D\Delta)\xi(\mathbf{x}, t) + \beta(\mathbf{x}, t)\xi_\tau(\mathbf{x}, t), \quad (3)$$

with $\xi_\tau(\mathbf{x}, t)$ as defined in Eq. (2) and

$$\begin{aligned} \alpha(\mathbf{x}, t) &= \left. \frac{\partial f(u, u_\tau)}{\partial u} \right|_{u=\bar{u}, u_\tau=\bar{u}_\tau}, \\ \beta(\mathbf{x}, t) &= \left. \frac{\partial f(u, u_\tau)}{\partial u_\tau} \right|_{u=\bar{u}, u_\tau=\bar{u}_\tau}. \end{aligned} \quad (4)$$

Equation (3) holds for infinitesimal small perturbations of the reference solution $\bar{u}(\mathbf{x}, t)$. Depending on the shape of the reference solution $\bar{u}(\mathbf{x}, t)$, different methods for the stability analysis are used.

A. Fourier space formulation

For spatially homogeneous solutions $\bar{u}(\mathbf{x}, t) = \bar{u}(t)$ the diffusion term vanishes and the dynamics can be characterized by

$$\dot{u}(t) = f(u(t), u_\tau(t)), \quad (5)$$

which is a delay differential equation (DDE) without spatial degrees of freedom. The solution of Eq. (5) can be obtained via numerical integration [35]. These solutions are equivalent to the homogeneous solutions of the spatially extended system Eq. (1). Note that in networks of coupled dynamical systems homogeneous solutions are known as synchronized solutions and the submanifold defined by Eq. (5) is known as a synchronization manifold [36].

While homogeneous solutions $u(t)$ of the spatially extended system within the synchronization manifold can be described by the scalar DDE Eq. (5), perturbations can be spatially homogeneous (tangential perturbations) or spatially heterogeneous (transversal perturbations). For homogeneous solutions the coefficients $\alpha(\mathbf{x}, t) = \alpha(t)$, $\beta(\mathbf{x}, t) = \beta(t)$ for the dynamics of the perturbations are spatially translation invariant and the Fourier basis can be used to diagonalize the Laplace operator. The n -dimensional Fourier transform $\hat{\xi}(\mathbf{k}, t)$ of the perturbations $\xi(\mathbf{x}, t)$ is defined by

$$\hat{\xi}(\mathbf{k}, t) = \int_{-\infty}^{\infty} \xi(\mathbf{x}, t) e^{-i\mathbf{k}\mathbf{x}} d\mathbf{x}, \quad (6)$$

where \mathbf{k} is the wave vector. In Fourier space Eq. (3) for perturbations of spatially homogeneous solutions can be written as

$$\frac{\partial \hat{\xi}(\mathbf{k}, t)}{\partial t} = (\alpha(t) - Dk^2)\hat{\xi}(\mathbf{k}, t) + \beta(t)\hat{\xi}_\tau(\mathbf{k}, t), \quad (7)$$

where $k = |\mathbf{k}|$ is the wave number corresponding to the wave vector \mathbf{k} . In fact, the original linear delay partial differential equation (3) is reduced via application of the Fourier transform to the DDE Eq. (7) without spatial extension but with the additional parameter k . The counterpart of Eq. (7) in network dynamics is known as the master stability function, where $-k^2$ are the eigenvalues of the Laplace operator and $\hat{\xi}(\mathbf{k}, t)$ are the corresponding eigenmodes [37]. The n Fourier modes $\hat{\xi}(\mathbf{k}, t)$ with $k = 0$ characterize the temporal evolution of

homogeneous perturbations within the synchronization manifold, whereas the Fourier modes with $k > 0$ specify spatially heterogeneous perturbations, i.e., transversal perturbations.

As can be seen from Eq. (7), the linear stability of the perturbations depends only on the wave number k but not on the specific form of the wave vectors \mathbf{k} . Thus, for the linear stability analysis it is reasonable to consider a continuous scalar parameter k , although boundary conditions and their symmetry may select a discrete subset of wave vectors \mathbf{k} . Moreover, the specific shape of the boundary conditions may become relevant for the nonlinear behavior of diffusion-induced instabilities. The transformation of the Fourier modes from \mathbf{k} space back to the original \mathbf{x} space can be done by an n -dimensional inverse Fourier transform

$$\xi(\mathbf{x}, t) = \frac{1}{(2\pi)^n} \int_{-\infty}^{\infty} \hat{\xi}(\mathbf{k}, t) e^{i\mathbf{k}\mathbf{x}} d\mathbf{k}. \quad (8)$$

B. Spatially homogeneous solutions

If the stability of a spatially homogeneous equilibrium point $\bar{u}(\mathbf{x}, t) = u^*$ is studied, the coefficients of the linearized DDE, Eq. (3), are time and space invariant, $\alpha(\mathbf{x}, t) = \alpha$, $\beta(\mathbf{x}, t) = \beta$. If, in addition, a time-invariant delay distribution is considered, $\rho(t, \tau) = \rho(\tau)$, the perturbations are described by a linear autonomous DDE. Thus, the exponential ansatz $\hat{\xi}(\mathbf{k}, t) = \hat{\xi}_k e^{st}$ can be used for the time evolution of the perturbations, where $\hat{\xi}_k = \hat{\xi}(\mathbf{k}, 0)$ are the Fourier modes at the initial time $t = 0$. By putting the exponential ansatz into Eq. (7), one obtains the characteristic equation

$$s = (\alpha - Dk^2) + \beta g(s). \quad (9)$$

The function $g(s)$ is the generally complex-valued Laplace transform of the delay distribution [38]

$$g(s) = \int_{\tau_{\min}}^{\tau_{\max}} \rho(\tau) e^{-s\tau} d\tau. \quad (10)$$

In general, Eq. (9) is a transcendental equation and has infinitely many roots s for each Fourier mode with wave number k . The infinitely many roots for a fixed wave number k indicate the infinite dimension due to the time delay, whereas the infinite dimension due to the spatial extension is covered by the parameter k , which can become arbitrarily large. The characteristic roots $s_l(k) = \lambda_l(k) + i\omega_l(k)$, i.e., the roots of Eq. (9), determine the temporal asymptotic behavior of the Fourier modes. The root with the largest real part $\lambda_l(k)$ is written simply as $s(k) = \lambda(k) + i\omega(k)$ and $\lambda(k)$ is called the maximal stability exponent (MSE). If the MSE $\lambda(k)$ is positive (negative), the amplitude of the corresponding Fourier mode increases (decreases) in time. The frequency of the oscillation of the Fourier mode in time is characterized by the imaginary part $\omega(k)$. The MSE $\lambda(k)$ can be used to find diffusion-induced instabilities. If the system is stable with respect to homogeneous perturbations $\lambda(0) < 0$ but unstable for heterogeneous perturbations $\lambda(k_u) > 0$, with some finite wave number $k_u > 0$ a diffusion-induced instability occurs. If, in addition, the imaginary part of the MSE at the instability is zero $\omega(k_u) = 0$, a classical Turing instability appears, whereas for $\omega(k_u) \neq 0$ the instability is called wave instability. For the computation of the stability border in parameter space the D-subdivision method can be used. The D-curves are

the boundaries in parameter space, where the real part of one characteristic root vanishes $\lambda_l(k) = 0$ [39]. They can be determined via Eq. (9). There are infinitely many D-curves for a specific wave number k . The stability border is specified by the D-curve with vanishing MSE $\lambda(k) = 0$, where, consequently, all other characteristic roots have a negative real part.

For the nonautonomous case, for example, for a homogeneous periodic solution, the calculation of the MSE $\lambda(k)$ can be no longer done via the characteristic Eq. (9). In this case a numerical method is used. In particular, the delay interval is discretized, where the step size $\Delta t = t_i - t_{i-1}$ for the discrete time steps $t_i = i\Delta t$ is chosen in such a manner that the maximum delay τ_{\max} is a multiple of the step size Δt . After discretization the state space of system (7) is finite and can be defined by the $(\frac{\tau_{\max}}{\Delta t})$ -dimensional vector,

$$\hat{\mathbf{E}}(\mathbf{k}, t_i) = [\hat{\xi}(\mathbf{k}, t_i), \hat{\xi}(\mathbf{k}, t_{i-1}), \dots, \hat{\xi}(\mathbf{k}, t_i - \tau_{\max})]^T, \quad (11)$$

where T denotes transposition. The state can be evolved by a discrete version of Eq. (7), which can be obtained, for example, via the semidiscretization method [40]. From the asymptotic behavior of the state of the perturbations, the MSE can be calculated numerically as [41]

$$\lambda(k) = \lim_{t \rightarrow \infty} \frac{1}{t} \ln \frac{|\hat{\mathbf{E}}(\mathbf{k}, t)|}{|\hat{\mathbf{E}}(\mathbf{k}, 0)|}. \quad (12)$$

By varying the wave number k in the discrete version of Eq. (7), the function $\lambda(k)$ can be obtained.

C. Analytical results

In this section, we give analytical results for the time-invariant case with a single discrete delay τ_0 . Putting the delay kernel $\rho(t, \tau) = \delta(\tau - \tau_0)$ for a single delay in Eq. (10) yields $g(s) = e^{-s\tau_0}$ and the characteristic Eq. (9) becomes

$$s = (\alpha - Dk^2) + \beta e^{-s\tau_0}. \quad (13)$$

Equation (13) can be written in the form $W(z)e^{W(z)} = z$. The function $W(z)$ is called the Lambert W function and has multiple branches for complex z [42]. With the Lambert W function the characteristic roots s of Eq. (13) can be calculated explicitly by

$$s = (\alpha - Dk^2) + \frac{W(\beta\tau_0 e^{(Dk^2 - \alpha)\tau_0})}{\tau_0}. \quad (14)$$

As an example, we use the Fisher-KPP equation with single discrete delay $\tau_0 = 1$ and $a = 1$:

$$\frac{\partial u(\mathbf{x}, t)}{\partial t} = au(\mathbf{x}, t)(1 - u_\tau(\mathbf{x}, t)) + D\Delta u(\mathbf{x}, t). \quad (15)$$

For the homogeneous equilibrium $u^* = 1$ of Eq. (15) the coefficients of the linearized DDE Eq. (7) are $\alpha = 0$ and $\beta = -a$. In Fig. 1 we show the real part of the first branch of the Lambert W function Eq. (14) (black solid), which is equal to the MSE $\lambda(k)$ of the equilibrium u^* . The analytically obtained MSE is compared with the numerical results from Sec. II B, where two different step sizes Δt were used. One can see that the deviations between the numerical and the analytical results are very small and they decrease for decreasing step size Δt .

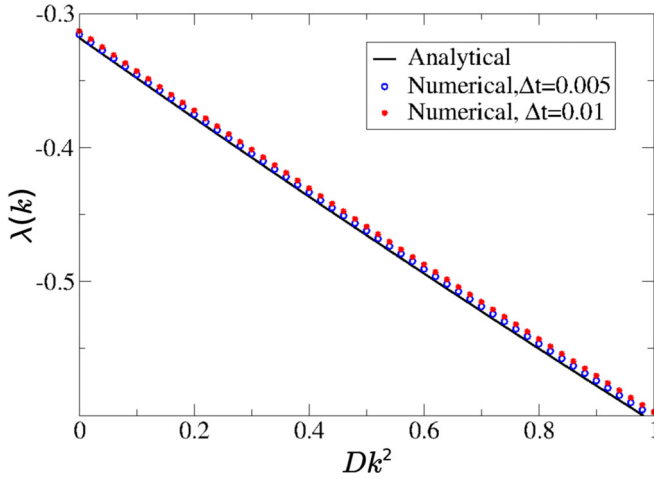


FIG. 1. The analytical results for the MSE λ of the equilibrium $u^* = 1$ of Eq. (15) coincide very well with our numerical results ($a = 1, \tau_0 = 1$).

D. Spatially heterogeneous solutions

In Sec. V the stability of arbitrary reference solutions of Eq. (1) is studied. In general, these solutions are spatially heterogeneous. We have calculated asymptotic solutions $\bar{u}(\mathbf{x}, t)$ of Eq. (1) with the forward-time central-space (FTCS) scheme [43]. The use of the FTCS method with discrete times $t_i = i\Delta t$ and the spatial grid points $\mathbf{x}_j, j = 1, \dots, n$ transforms the spatially extended time-delay system with an infinite-dimensional state space to a system of ordinary differential equations with a finite-dimensional state space.

The FTCS method can also be used to determine the solution of the linear system Eq. (3). The finite-dimensional approximation of the state of the linearized system Eq. (3) can be defined by the $(n \frac{\tau_{\max}}{\Delta t})$ -dimensional vector

$$\begin{aligned} \Xi(t_i) = & [\xi(\mathbf{x}_1, t_i), \dots, \xi(\mathbf{x}_n, t_i), \\ & \xi(\mathbf{x}_1, t_{i-1}), \dots, \xi(\mathbf{x}_n, t_{i-1}), \\ & \vdots \\ & \xi(\mathbf{x}_1, t_i - \tau_{\max}), \dots, \xi(\mathbf{x}_n, t_i - \tau_{\max})]^T. \end{aligned} \quad (16)$$

Similar to Eq. (12), the stability of the system can be calculated by the asymptotic behavior of the perturbations

$$\Lambda = \lim_{i \rightarrow \infty} \frac{1}{t_i} \ln \frac{|\Xi(t_i)|}{|\Xi(0)|}. \quad (17)$$

In Eq. (17) Λ is called the maximal Lyapunov exponent (MLE). not to be confused with the MSE $\lambda(k)$ in Eq. (12). Whereas the MSE $\lambda(k)$ characterizes the stability of homogeneous solutions against perturbations with wave number k , the MLE Λ characterizes the stability of an arbitrary asymptotic solution of Eq. (1). Moreover, the MLE does not depend on the wave number k . In fact, the information on the shape of the most unstable perturbation is contained in the vector $\Xi(t_i)$, which approximates the most dominant Lyapunov vector corresponding to the asymptotic solution of Eq. (1).

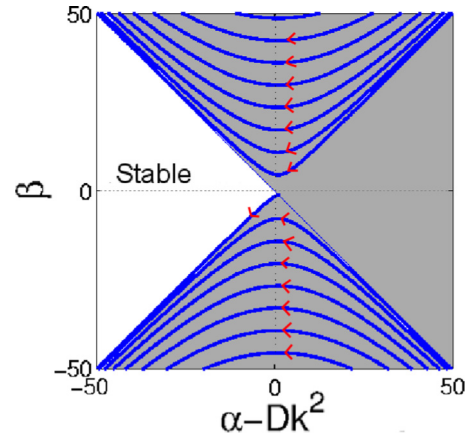


FIG. 2. D-curves of Eq. (18) for $\tau_0 = 1$. The (red) arrows indicate the direction of the D-curve with increasing ω . No Turing or wave instability is possible (see text).

III. RESULTS FOR CONSTANT DELAYS

In this section the results for the existence of diffusion-driven instabilities from homogeneous equilibria of reaction-diffusion systems with constant discrete and distributed delay are presented.

A. Single discrete delays

The D-subdivision method [39] is used to study diffusion-driven instabilities in a general one-component system with a single discrete delay τ_0 . The D-curves in (α, β) parameter space are derived by substituting $s = i\omega$ in Eq. (13),

$$\left. \begin{aligned} \beta &= Dk^2 - \alpha, & \text{for } \omega = 0, \\ \alpha - Dk^2 &= \frac{\omega}{\tan \omega \tau_0}, \\ \beta &= -\frac{\omega}{\sin(\omega \tau_0)}, \end{aligned} \right\} \text{for } \omega > 0. \quad (18)$$

It is sufficient to consider only non-negative frequencies $\omega \geq 0$ because according to Eq. (13), the D-curves for $s = i\omega$ and the complex conjugate $\bar{s} = -i\omega$ are the same. Without loss of generality, by rescaling the parameters α, β , and D the discrete delay can be set to 1, $\tau_0 = 1$. The D-curves are shown in Fig. 2. Each curve is associated with frequencies in one subinterval $\omega \in [(m-1)\pi, m\pi]$, where $m \in \mathbb{N}$ is odd (even) for the curves with $\beta < 0$ ($\beta > 0$). The (red) arrows on the D-curves indicate the direction of increasing ω . The system is stable in the white region of the parameter plane.

A diffusion-driven instability is possible if the system is stable for $k = 0$ and unstable for some $k > 0$. This can be illustrated as follows. We consider an arbitrary stable homogeneous state in the white region of Fig. 2 with fixed parameters α, β , and $k = 0$. Then, a diffusion-driven instability is possible, if for increasing k or decreasing $\alpha - Dk^2$, respectively, one crosses a D-curve and reaches an unstable region. Obviously, this is not possible for the D-curves in Fig. 2, which means that Turing or wave instabilities do not exist in single-species reaction-diffusion systems with a discrete constant delay. This can be proven by showing that the D-curves for a single discrete delay do not intersect each other and by deriving the monotonic

relationship between the α and β values for the two D-curves that separate stable and unstable regions. However, a rigorous mathematical proof for this is out of the scope of this paper.

B. Distributed delays

For distributed delays the Laplace transform of the delay distribution at the D-curves can be written as $g(i\omega) = \hat{g}(\omega)e^{i\gamma(\omega)}$, where $\hat{g}(\omega)$ and $\gamma(\omega)$ are the amplitude and the phase of the function g , respectively. With this definition the D-curves in parameter space can be determined by

$$\left. \begin{aligned} \beta &= Dk^2 - \alpha, & \text{for } \omega = 0, \\ \alpha - Dk^2 &= -\frac{\omega}{\tan(\gamma(\omega))}, \\ \beta &= \frac{\omega}{\hat{g}(\omega)\sin(\gamma(\omega))}, & \text{for } \omega > 0. \end{aligned} \right\} \quad (19)$$

Again, no negative frequencies are considered because, according to Eq. (10) we have $g(i\omega) = \bar{g}(-i\omega)$, and consequently, no additional D-curves appear for $\omega < 0$. For the case of a single discrete delay we have $\hat{g}(\omega) = 1$ and $\gamma(\omega) = -\omega\tau_0$, and obviously, Eq. (19) is identical to Eq. (18). In general, for a distributed delay both the amplitude \hat{g} and the phase γ depend on the frequency ω . However, according to the normalization of the delay distribution ρ we have $g(0) = 1$. This is the reason why the D-curve $\beta = Dk^2 - \alpha$ for $\omega = 0$ is independent of the delay. Moreover, it is strictly monotonically decreasing, which means that for an arbitrary single-species reaction-diffusion systems with an arbitrary constant delay distribution no classical Turing instability with $\omega = 0$ is possible.

As can be derived from Eq. (10), for a symmetric delay distribution around the mean delay τ_m with $\rho(\tau_m + \tau) = \rho(\tau_m - \tau)$ the amplitude of the function $g(i\omega)$ is given by (see Appendix)

$$\hat{g}(\omega) = 2 \left| \int_{\tau_m}^{\tau_{\max}} \rho(\tau) \cos \omega(\tau - \tau_m) d\tau \right|. \quad (20)$$

The phase is $\gamma(\omega) = -\omega\tau_m$ or $\gamma(\omega) = \pi - \omega\tau_m$ for a positive or negative value of the integral in Eq. (20), respectively. As a consequence, the parametric curve for α in Eq. (19) does not depend on the delay distribution and the condition $\frac{d\alpha}{d\omega} \leq 0$ holds for the derivative of the parametric function. This might be a reason why in our extensive numerical studies with various symmetrical delay distributions no diffusion-driven instabilities for one-component reaction-diffusion systems were detected. However, in this case a possible proof is much more complex because, in contrast to the case of a single discrete delay, for distributed delays the varying amplitude $\hat{g}(\omega)$ of the function g is not constant, meaning that different D-curves can intersect each other.

In case of an asymmetric delay distribution the phase $\gamma(\omega)$ can adopt arbitrary values, and therefore, the condition $\frac{d\alpha}{d\omega} \leq 0$ no longer holds. As a consequence, loops of the D-curves are also possible. An appropriate example for the loops is shown in Fig. 3, where the asymmetric delay distribution $\rho(\tau) = 0.7\delta(\tau - 0.48) + 0.3\delta(\tau - 1.52)$ was used. The crucial loop for the existence of a wave instability is enlarged in Fig. 3(b). The nonmonotonic behavior of the D-curve, which separates stable from unstable regions, enables the occurrence of a diffusion-induced instability. In this case, the nonmonotonic

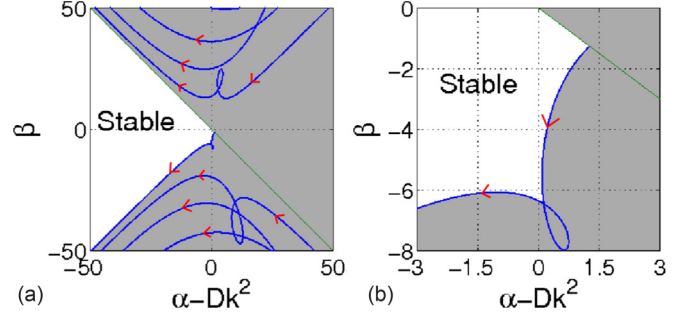


FIG. 3. D-curves of Eq. (19) with an asymmetric delay distribution $\rho(\tau) = 0.7\delta(\tau - 0.48) + 0.3\delta(\tau - 1.52)$. Panel (b) is an enlarged figure of panel (a) and shows the parameter region, where a wave instability is possible. The red arrows indicate the direction of the D-curves with increasing ω .

behavior of the D-curve is associated with a sign change of the derivative $\frac{d\alpha}{d\omega}$, which becomes partially larger than zero in the region of the loop. In fact, in the valley of the D-curve for $\alpha = 0$ and $-6.2 < \beta < -6$ the equilibrium is stable against homogeneous perturbations with $k = 0$ and becomes unstable against spatially heterogeneous perturbations with wave number $k > 0$. As a result, asymmetric delay distributions in single-species reaction-diffusion systems can lead to diffusion-induced instabilities from equilibria.

IV. RESULTS FOR TIME-VARYING DELAYS

In this section, diffusion-induced instabilities of the homogeneous equilibrium $u^* = 1$ for systems with time-varying delays are studied. In this case small perturbations are described by a linear DDE (3) with constant coefficients α , β , and the time-varying delay distribution

$$\rho(t, \tau) = \delta(\tau - \tau_0(t)). \quad (21)$$

The Fisher-KPP equation (15) with periodic time-varying delay is used for the following numerical examples. For periodic delays the Floquet theory is valid and the MSE $\lambda(k)$ is equivalent to the real part of the dominant Floquet exponent. The coefficients of the linearized system are $\alpha = 0$ and $\beta = -a$. Two different types of periodic delay variations are considered. The first is a rectangular delay,

$$\tau_0(t) = \begin{cases} \tau_m - \tau_A, & \text{if } t \bmod T_p < T_1 \\ \tau_m + \tau_A, & \text{otherwise,} \end{cases} \quad (22)$$

and the second is a sinusoidal delay,

$$\tau_0(t) = \tau_m + \tau_A \sin\left(\frac{2\pi t}{T_p}\right), \quad (23)$$

where τ_A and T_p are the amplitude and the period of the delay variation. For the rectangular delay the switching time $T_1 < T_p$ is used to implement an asymmetric delay variation.

In Fig. 4 the MSE $\lambda(k)$ of the Fisher-KPP equation with an asymmetrically rectangular delay is shown for varying periods T_p . The parameters $\tau_m = 1$, $\tau_A = 0.52$, and a longer duration of the short delay $T_1 = 0.7T_p$ are chosen. The parameter $a = -\beta = 6.1$ corresponds to the valley of the D-curve of

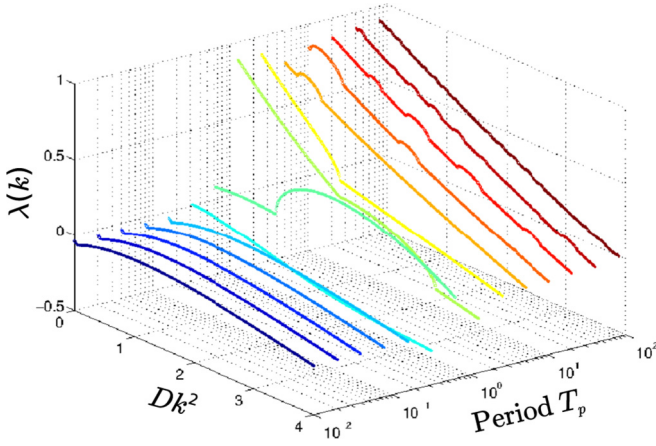


FIG. 4. MSE $\lambda(k)$ for different periods T_p of a rectangular delay fluctuation Eq. (22). Two limiting cases for slowly and fast time-varying delay can be identified, i.e., large and small periods T_p , respectively.

the system with distributed delay, where a wave instability appears [cf. Fig. 3(b)]. From Fig. 4 an asymptotic behavior for the two limiting cases of a very slow ($T_p \rightarrow \infty$) and fast ($T_p \rightarrow 0$) delay variation can be identified, which is studied semianalytically in the next sections.

A. Slowly time-varying delays

By using Floquet theory the solution of the linear DDE equation, Eq. (7), with constant coefficients α , β and a periodic delay distribution $\rho(t, \tau) = \rho(t - T_p, \tau)$ can be written as [44]

$$\hat{\xi}(\mathbf{k}, t) = \sum_{l=0}^{\infty} \hat{\xi}_l(\mathbf{k}, t) e^{\mu_l(\mathbf{k})t}, \quad (24)$$

where $\hat{\xi}_l(\mathbf{k}, t)$ is a time-periodic coefficient vector with $\hat{\xi}_l(\mathbf{k}, t) = \hat{\xi}_l(\mathbf{k}, t + T_p)$ and $\mu_l(\mathbf{k})$ is called the Floquet exponent. Since Eq. (7) is a time-delay system, in general, infinitely many Floquet modes exist. The frozen time approach can be used to analyze the stability of the nonautonomous DDE for slowly time-varying delays [45].

In particular, the period T_p of the delay variation is separated into P time intervals $I_j = [t_{j-1}, t_j]$ with $t_j = j\Delta t$ and $t_p = T_p$. This is similar to the discretization used in Sec. II D for the numerical methods, but here we consider a larger step size $\tau_{\max} < \Delta t \ll T_p$. Note that the inequality $\tau_{\max} \ll T_p$ holds for slowly time-varying delays. As a consequence, the variation of the delay distribution within one interval I_j is negligible, i.e., the constant delay distribution $\rho(t, \tau) = \rho(t_j, \tau)$ can be used for $t \in I_j$. In this case the perturbations $\hat{\xi}(\mathbf{k}, t)$ within the intervals I_j can be described by the linear autonomous DDE Eq. (7) with the constant delay distribution $\rho(t_j, \tau)$. This means that the solution in the j th interval I_j is described by the infinitely many eigenmodes $e^{s_l^j(\mathbf{k})t}$, where $s_l^j(\mathbf{k}) = \lambda_l^j(\mathbf{k}) + i\omega_l^j(\mathbf{k})$, with $l = 0, \dots, \infty$ being the characteristic roots of the autonomous DDE [46,47]. The characteristic roots $s_l^j(\mathbf{k})$ can be calculated via the characteristic Eq. (9) with the corresponding constant delay distribution $\rho(t_j, \tau)$. By using the adiabatic theorem [48], which states

that for slowly time-varying systems the coefficient for the l th eigenmode $e^{s_l^j(\mathbf{k})t}$ in the present interval I_j is the same coefficient as for the l th eigenmode $e^{s_l^{j-1}(\mathbf{k})t}$ from the previous interval I_{j-1} , one can show that the Floquet exponents μ_l can be approximated by [45,47]

$$\mu_l(\mathbf{k}) = \lambda_l(\mathbf{k}) + i\omega_l(\mathbf{k}) = \frac{1}{P} \sum_{j=1}^P s_l^j(\mathbf{k}). \quad (25)$$

Thus, for slowly time-varying delays the MSE $\lambda(k)$ is the time average of the real part $\lambda_0^j(k)$ of the dominant characteristic exponents $s_0^j(k)$ of the time-invariant systems with the frozen delay distributions $\rho(t_j, \tau)$, $j = 1, \dots, P$. Similar to the analysis in Sec. III A for a time-invariant discrete delay, no diffusion-induced instabilities are possible for a slowly time-varying discrete delay because from the Lambert W approach Eq. (14) it follows that the real parts $\lambda_0^j(k)$ of the dominant exponents in each interval, $j = 1, \dots, P$, become smaller for increasing wave number k .

The MSE $\lambda(k)$ of the KPP-Fisher Eq. (15) with rectangular delay fluctuation and large periods T_p is shown in Fig. 5(a). The parameters are equivalent to the parameters used in Fig. 4. The relationship between the MSE $\lambda(k)$ and Dk^2 is approximately linear. For an increasing period T_p the MSE $\lambda(k)$ for the system with fluctuating delay approaches the limiting case of the frozen time approximation (black, solid line), calculated with Eq. (25).

B. Fast time-varying delays

If the period T_p of the delay fluctuation is much smaller than the internal time scale of the system, the original moving Dirac- δ peak in Eq. (21) can be replaced by a time-averaged invariant delay distribution [38]

$$\bar{\rho}(\tau) = \frac{1}{T_p} \int_t^{t+T_p} \delta(\tau - \tau_0(t')) dt'. \quad (26)$$

This means that the solution $\hat{\xi}(\mathbf{k}, t)$ does not change significantly in the time interval $[t, t + T_p]$. As a consequence, the time evolution of the Fourier modes $\hat{\xi}(\mathbf{k}, t)$ of the nonautonomous Eq. (7) can be approximated by the exponential behavior $\hat{\xi}(\mathbf{k}, t) = \hat{\xi}_k e^{st}$ of the autonomous distributed delay comparison system

$$\frac{\partial \hat{\xi}(\mathbf{k}, t)}{\partial t} = (\alpha - Dk^2) \hat{\xi}(\mathbf{k}, t) + \beta \int_{\tau_{\min}}^{\tau_{\max}} \bar{\rho}(\tau) \hat{\xi}(\mathbf{k}, t - \tau) d\tau. \quad (27)$$

The distributed delay comparison system Eq. (27) can be analyzed via the characteristic Eq. (9) and the D-subdivision method as described in Sec. II A.

In Fig. 5(b) the MSE $\lambda(k)$ is shown for small periods T_p of the delay variation. The parameters are equivalent to the parameters in Fig. 4. The black solid line represents the asymptotic behavior for infinitely small periods, $T_p \rightarrow 0$, calculated by the distributed delay comparison system Eq. (27). For $T_p = 0.32$ (green dashed line) the behavior of the MSE $\lambda(k)$ is not related to the results of the distributed delay

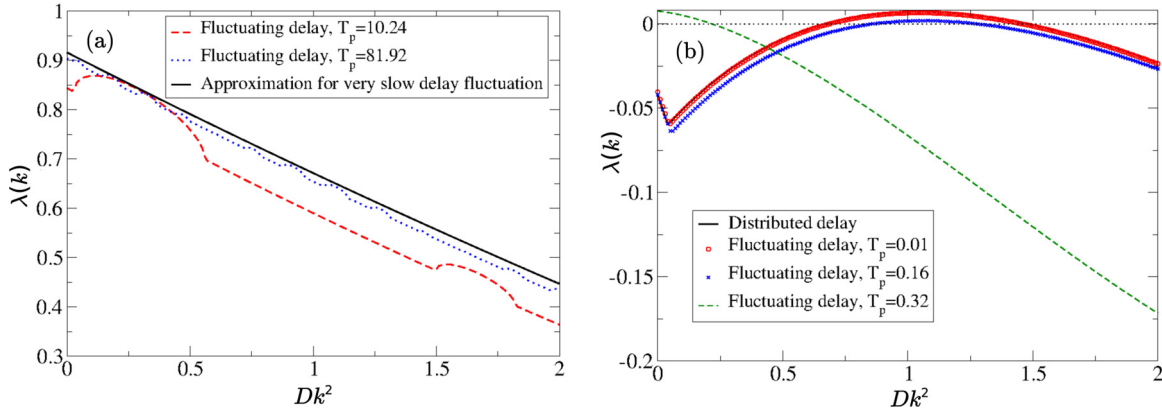


FIG. 5. Convergence of the MSE $\lambda(k)$ for the two limiting cases of a (a) slow and (b) fast delay fluctuation. The same parameters as in Fig. 4 are used.

comparison system because there are still significant changes of the solution $\hat{\xi}(\mathbf{k}, t)$ in the time interval $[t, t + T_p]$. However, for smaller periods ($T_p = 0.16$: blue crosses; $T_p = 0.01$: red circles) the MSE gets closer to the MSE of the distributed delay comparison system.

In this example with a rectangular delay Eq. (22) with $\tau_m = 1$, $\tau_A = 0.52$, and $T_1 = 0.7T_p$, a wave instability is possible for a fast asymmetric delay fluctuation with $T_p \leq 0.16$. The MSE $\lambda(k)$ is negative for $k = 0$ and has a positive maximum near $Dk^2 \approx 1$, i.e., at a finite wave number $k_u > 0$ [cf. Fig. 5(b)]. The time-averaged delay distribution defined by Eq. (26), $\bar{\rho}(\tau) = 0.7\delta(\tau - 0.48) + 0.3\delta(\tau - 1.52)$, is to the asymmetric delay distribution that was used in Fig. 3. Moreover, the parameter $a = -\beta = 6.1$ of the example is chosen in the valley of the D-curve, where the wave instability is possible for the system with distributed delay. Thus, it is not surprising that the wave instability occurs also for fast time-varying delays. For the distributed delay with $T_p \rightarrow 0$ the maximum of the MSE is located at $Dk_u^2 = 1.05$, which corresponds to the MSE $\lambda(k_u) = 0.0074$ and a frequency $\omega(k_u) = 4.564$. Indeed, the diffusion-induced instability is a wave instability and not a classical Turing instability, because the frequency of the Fourier mode is nonzero. Wave instabilities can be found, for example, in chemical reaction-diffusion systems or in the convection of binary mixtures [3,49]. In nondelayed reaction-diffusion systems Turing noted that for the existence of a wave instability at least three species are necessary and the resulting pattern will be of the form of “genuine traveling waves” [1].

An example of the corresponding oscillatory Turing pattern in one space dimension with periodic boundary condition is shown in Fig. 6. The Fisher-KPP Eq. (15) with $a = 6.1$, $D = 0.1$ and the asymmetrically distributed delay is used. Indeed, one can observe a traveling wave. The wave number $k_s = 3.1$ and the angular frequency $\omega_s = 4.6$ of the structure are near the corresponding wave number $k_u = \sqrt{10.5}$ and the frequency $\omega(k_u) = 4.564$ of the linear stability analysis. In snapshots of the two-dimensional structure with periodic boundary conditions, which are shown in Fig. 7, at first one observe some spots [see panel (a) and (b)] and later the spots evolve into stripes [see panel (c) and (d)]. The dark stripes can be found at different locations in panels (c) and (d), which indicate a traveling wave solution.

C. General time-varying delays

If the behavior of the time-varying delay cannot be approximated by the limiting cases of a slow or fast delay variation, no general statement on the occurrence of diffusion-driven instabilities can be made. To investigate the occurrence of a Turing or wave instability, one can compare the MLE of the asymptotic solution for the delayed reaction-diffusion systems with and without diffusion.

In Fig. 8 the MLE Λ of the Fisher-KPP Eq. (15) with a sine-shaped delay is shown. In this section we are only interested in instabilities from homogeneous equilibria, which corresponds to the region on the left-hand side of the bifurcation point. In particular, in this parameter region the asymptotic state of the system without diffusion (solid black) is the stable homogeneous equilibrium $u^* = 1$ with $\Lambda < 0$. If the system with diffusion $D > 0$ converges to the same equilibrium, the MLE is identical to the system without diffusion. In Fig. 8, the red dashed line for $D = 0.05$ coincides with the black curve for $D = 0$. Numerical integration of Eq. (15) for values of a on the left of the bifurcation point showed that, in fact, the system converges for both cases $D = 0$ and $D = 0.05$ to the same homogeneous equilibrium $u^* = 1$ and not to another attractor with the same or nearly the same MLE. Similar results were obtained for a symmetric rectangular

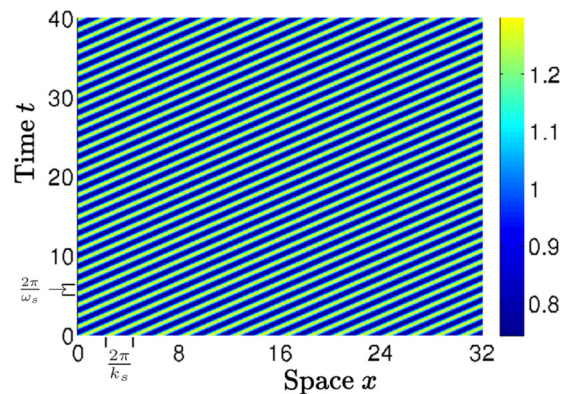


FIG. 6. 1D-Turing pattern for the system Eq. (15) with the distributed delay $\rho(\tau) = 0.7\delta(\tau - 0.48) + 0.3\delta(\tau - 1.52)$ and periodic boundary condition ($a = 6.1, D = 0.1$).

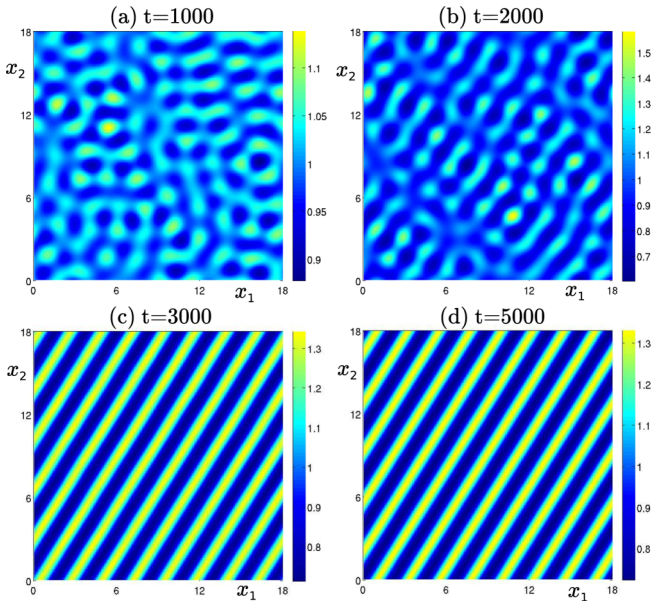


FIG. 7. Snapshots of 2D-Turing pattern for the system Eq. (15) with the distributed delay $\rho(\tau) = 0.7\delta(\tau - 0.48) + 0.3\delta(\tau - 1.52)$ and periodic boundary conditions ($a = 6.1, D = 0.1$). The snapshots are taken at (a) $t = 1000$, (b) $t = 2000$, (c) $t = 3000$, and (d) $t = 5000$. The size of space is 18×18 . An initial condition near the equilibrium $u^* = 1$ with an arbitrary small perturbation was used.

delay with $\tau_m = 1.5, \tau_A = 0.5, T_p = 2$, and $T_1 = 1$, which are not shown in the paper. In our research we have made various numerical calculations for different parameters and symmetrical delay fluctuations. But so far, we have not found any wave instability from equilibria in cases with symmetrical time-varying delay, which conforms with the observations for systems with symmetric delay distributions.

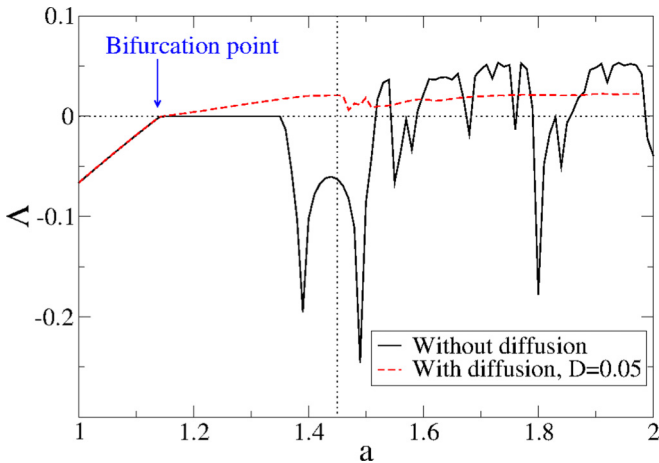


FIG. 8. MLE Λ of Eq. (15) for $D = 0$ (black) and $D = 0.05$ (red dashed) dependent on the parameter a . A sine-shaped delay with $\tau_m = 1.5, \tau_A = 0.5$, and $T_p = 2\pi^2$ is used. Periodic boundary conditions and random initial conditions near the equilibrium $u^* = 1$ are considered. The space size is 10.

V. DIFFUSION-INDUCED INSTABILITIES FROM PERIODIC ORBITS

In general, Turing instabilities are studied from stable equilibria. In 1982, Lin and Kahn studied the stability of homogeneous limit cycles in the presence of diffusion [13]. For limit cycles the MLE is associated with perturbations along the trajectory and vanishes, $\Lambda = 0$. For Eq. (15) with constant discrete delay τ_0 the homogeneous periodic orbit that exists for $a\tau_0 > \pi/2$ has a zero MLE $\Lambda = 0$, similar to the limit cycles studied in [13]. In this case, diffusion-driven instabilities similar to the original Turing instability may be possible. Here, we are interested in the stability of such homogeneous periodic orbits of Eq. (15) against spatially heterogeneous perturbations in the case of time-varying delays. For time-varying delays the system becomes nonautonomous and periodic orbits with negative MLEs $\Lambda < 0$ are possible [50,51]. As a consequence, the comparison of the MLE for the system with diffusion and the system without diffusion maybe useful for finding diffusion-induced instabilities.

In Fig. 8 the MLE of Eq. (15) with sinusoidally varying delay is shown for varying parameter a . On the right-hand side of the bifurcation point one can find some windows with a stable solution ($\Lambda < 0$) for the Hutchinson equation (black, solid), i.e., Eq. (15) with variable delay but without diffusion. These solutions are windows with attracting periodic orbits. In some situations the MLE of the system with diffusion (red, dashed) is positive at the same value of the bifurcation parameter a . This is an indication for a stable homogeneous periodic orbit of the system without diffusion, which may become unstable in the presence of diffusion. For a detailed analysis, we choose $a = 1.45$ as a prototypical examples. The selected parameter is denoted by a vertical dotted line in Fig. 8.

We have calculated the MSE $\lambda(k)$ in dependence of the wave number k for this example. The results are shown in Fig. 9. The stable periodic solution in the system without diffusion is illustrated in Fig. 9(a). The period of the solution is equivalent to the period T_p of the periodic delay, which means that there is some resonance between the internal frequency of the Hutchinson equation and the driving frequency of the variable delay (see [52,53] and references therein). For this so-called mode-locked homogeneous solution the MSE $\lambda(k)$ is shown in Fig. 9(b). Obviously, one finds that the MSE is negative for $k = 0$ and positive for $Dk^2 \in [0.05, 0.24]$. This indicates a Turing-like diffusion-induced instability. The resulting spatiotemporal patterns in one space dimension are shown in Fig. 10 for two different diffusion coefficients $D = 0.01$ (a) and $D = 0.1$ (b). Obviously, the structures are standing waves with a period equal to the period T_p of the time-varying delay. Thus, the variable delay drives the system to a periodic state, which is stable for the case without diffusion but unstable in the presence of diffusion. The occurring structures are standing waves similar to the structures that were found in nondelayed reaction-diffusion systems with external periodic forcing [52]. The time-averaged spatial spectra of the standing waves are shown in Fig. 11 for the two cases with $D = 0.01$ and $D = 0.1$. Due to the periodic boundary conditions only a discrete spectrum appears. Since the MSE $\lambda(k)$ is positive in a specific interval for Dk^2 , a larger diffusion coefficient D leads to smaller wave number k in the observed pattern.

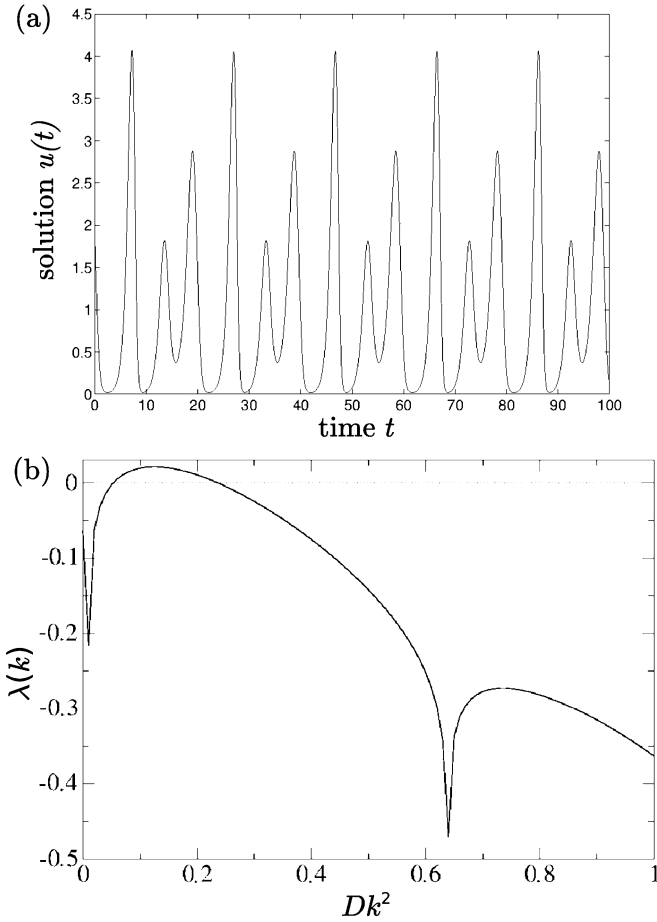


FIG. 9. (a) Periodic orbit for Hutchinson equation with a sine-shaped fluctuating delay with $\tau_m = 1.5$, $\tau_A = 0.5$, $T_p = 2\pi^2$, and $a = 1.45$. (b) The MSE $\lambda(k)$ for a spatial homogeneous state with the periodic orbit shown in (a).

In other words, the wavelength of the diffusion-induced pattern will be larger for larger D . In particular, the wave numbers $k \in [2.24, 4.90]$ for the system with $D = 0.01$ and $k \in [0.71, 1.55]$ for the system with $D = 0.1$ correspond to a positive MSE $\lambda(k)$ in the linear stability analysis. As can be seen from Fig. 11, the peaks with the maximal amplitude in the spatial spectra of the asymptotic solution of the nonlinear system are located in these intervals of positive MSEs.

VI. CONCLUSIONS

In this paper we have studied the occurrence of diffusion-driven instabilities in one-component reaction-diffusion systems with delay. In a system without delay more than one (two) component(s) is necessary for a Turing (wave) instability. We have shown that diffusion-driven instabilities are already possible in reaction-diffusion systems with only one component but with a delay in the reaction term. This is not a contradiction to former results, because a time delay increases the dimension of the system. Roughly speaking, a one-component system with delay can be interpreted as a system without delay but with infinitely many components, where only a single component diffuses.

The possibility of a diffusion-induced instability from equilibria of a one-component system with delayed reaction

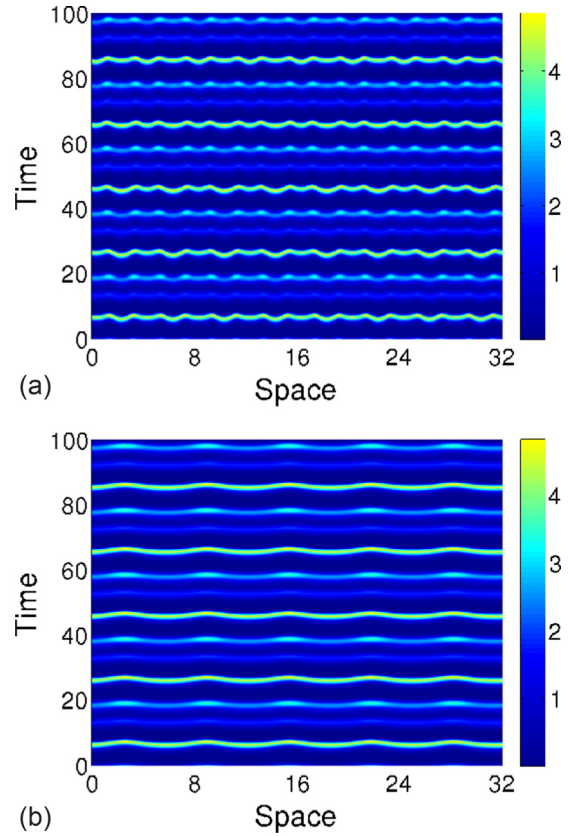


FIG. 10. Asymptotic state of Eq. (15) in case of a diffusion-driven instability for parameters as in Fig. 9 and (a) $D = 0.01$, (b) $D = 0.1$. Space size is 32, and periodic boundary conditions are considered. The initial condition is chosen close to the homogeneous periodic orbit in Fig. 9(a).

was studied systematically for various types of delays. For the case with a single time-invariant discrete delay a diffusion-induced instability from an equilibrium is not possible. For a symmetrically distributed delay, no diffusion-induced instability was found, but a rigorous proof has not been given. In contrast, for an asymmetric time-invariant delay distribution the existence of a wave instability was found. For time-varying delays, the stability of the system in the limiting cases of a slowly and fast varying delay was studied systematically and related to the autonomous cases with constant delays. On the one hand, a slow delay fluctuation can be approximated by the averaged stability behavior of several subsystems with constant frozen delays. In this case, a diffusion-driven instability is not possible. On the other hand, a fast delay fluctuation can be approximated by a distributed delay. As a consequence, a wave instability is possible for an asymmetrically time-varying delay. We have shown a simple argument as to why asymmetric delays in contrast to symmetric delays are more suitable for the generation of diffusion-driven instabilities.

In the case of a periodic delay, the system without diffusion can follow a stable periodic orbit with negative maximal Lyapunov exponent and a period equal to the period of the delay variation. In other words, the system is driven by the periodic delay and some resonance condition between the delay frequency and the internal frequency of the system is

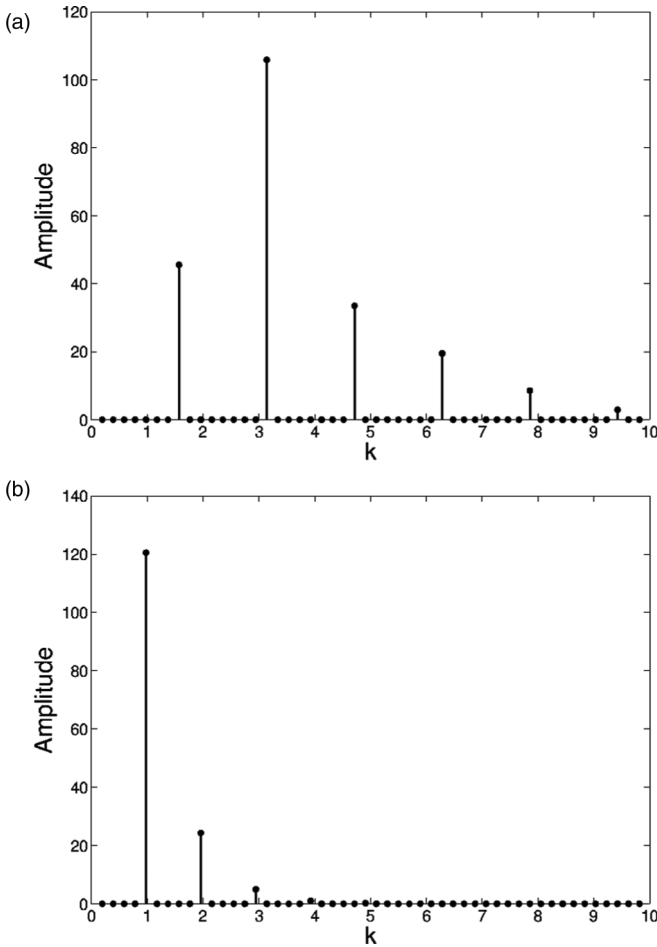


FIG. 11. Spatial spectrum for structures in Fig. 10 with (a) $D = 0.01$ and (b) $D = 0.1$. A larger diffusion coefficient leads to a larger wavelength of the structures. The dominant peaks are located at wave numbers where the MSE $\lambda(k)$ of the homogeneous periodic solution is positive; cf. Fig. 9(b).

fulfilled. Diffusion-driven instabilities from such mode-locked stable periodic orbits were found numerically. The period of the resulting standing waves are equal to the period of the variable delay, similar to the standing waves that were found in externally forced chemical reactions [52]. The wavelengths of the standing waves are close to the unstable Fourier modes of the linear stability analysis. A further investigation of the influence of asymmetric delay variations and asymmetrically distributed delays in reaction-diffusion systems and the investigation of the resulting pattern could be directions for future work.

APPENDIX: SYMMETRIC DELAY DISTRIBUTION

From Eq. (10) we have

$$g(i\omega) = \int_{\tau_{\min}}^{\tau_{\max}} \rho(\tau) e^{-i\omega\tau} d\tau. \quad (\text{A1})$$

A useful change of the integration variable leads to

$$g(i\omega) = e^{-i\omega\tau_m} \int_{\tau_{\min}-\tau_m}^{\tau_{\max}-\tau_m} \rho(\tau_m + \tau') e^{-i\omega\tau'} d\tau'. \quad (\text{A2})$$

For a symmetric delay distribution around the mean τ_m we get

$$g(i\omega) = e^{-i\omega\tau_m} \int_0^{\tau_{\max}-\tau_m} \rho(\tau_m + \tau') (e^{-i\omega\tau'} + e^{i\omega\tau'}) d\tau', \quad (\text{A3})$$

resulting in

$$g(i\omega) = e^{-i\omega\tau_m} 2 \int_0^{\tau_{\max}-\tau_m} \rho(\tau_m + \tau') \cos(\omega\tau') d\tau'. \quad (\text{A4})$$

By going back to the original integration variable we get

$$g(i\omega) = e^{-i\omega\tau_m} 2 \int_{\tau_m}^{\tau_{\max}} \rho(\tau) \cos(\omega(\tau - \tau_m)) d\tau'. \quad (\text{A5})$$

From Eq. (A5) we get the amplitude $\hat{g}(\omega)$ defined by Eq. (20) and the corresponding phase $\gamma(\omega)$.

-
- [1] A. M. Turing, *Philos. Trans. R. Soc. Lond. B* **237**, 37 (1952).
 [2] I. Prigogine and G. Nicolis, *Self-Organization in Non-Equilibrium Systems* (Wiley, New York, 1977).
 [3] A. M. Zhabotinsky, M. Dolnik, and I. R. Epstein, *J. Chem. Phys.* **103**, 10306 (1995).
 [4] A. B. Rovinsky and M. Menzinger, *Phys. Rev. Lett.* **69**, 1193 (1992).
 [5] B. Henry and S. Wearne, *Physica A* **276**, 448 (2000).
 [6] E. P. Zemskov, K. Kassner, M. J. B. Hauser, and W. Horsthemke, *Phys. Rev. E* **87**, 032906 (2013).
 [7] K. Ikeda, H. Daido, and O. Akimoto, *Phys. Rev. Lett.* **45**, 709 (1980).
 [8] J. Tlustý, A. Polacek, C. Danek, and J. Spacek, *Selbsterregte Schwingungen an Werkzeugmaschinen* (WEB Verlag Technik, Berlin, 1962); S. Tobias, *Machine Tool Vibration* (Blackie, London, 1965).
 [9] R. Bellman, *Adaptive Control Processes: A Guided Tour* (Princeton University Press, Princeton, NJ, 1961).
 [10] K. Pyragas, *Phys. Lett. A* **170**, 421 (1992).
 [11] L. Glass and M. C. Mackey, *From Clocks to Chaos, The Rhythms of Life* (Princeton University Press, Princeton, NJ, 1988).
 [12] D. J. Amit, *Modeling Brain Function: The World of Attractor Neural Networks* (Cambridge University Press, New York, 1989).
 [13] J. Lin and P. B. Kahn, *J. Math. Biol.* **13**, 383 (1982).
 [14] S. Busenberg and W. Huang, *J. Diff. Equ.* **124**, 80 (1996).
 [15] P. Ghosh, *Phys. Rev. E* **84**, 016222 (2011).
 [16] S. Chen and J. Shi, *J. Diff. Equ.* **253**, 3440 (2012).
 [17] M. Bestehorn, E. V. Grigorieva, and S. A. Kaschenko, *Phys. Rev. E* **70**, 026202 (2004).
 [18] S. Sen, P. Ghosh, and D. S. Ray, *Phys. Rev. E* **81**, 056207 (2010).
 [19] S. V. Gurevich and R. Friedrich, *Phys. Rev. Lett.* **110**, 014101 (2013).
 [20] A. Pimenov, A. G. Vladimirov, S. V. Gurevich, K. Panajotov, G. Huyet, and M. Tlidi, *Phys. Rev. A* **88**, 053830 (2013); S. V. Gurevich, *Philos. Trans. R. Soc. Lond. A* **372**, 20140014 (2014).
 [21] L. Ji and Q. S. Li, *J. Chem. Phys.* **123**, 094509 (2005).
 [22] K. P. Hadeler and S. Ruan, *Discrete Cont. Dyn. Sys. S* **8**, 95 (2007).

- [23] E. A. Gaffney and N. A. M. Monk, *Bull. Math. Biol.* **68**, 99 (2006); S. Seirin Lee, E. A. Gaffney, and N. A. M. Monk, *ibid.* **72**, 2139 (2010); S. Seirin Lee, E. A. Gaffney, and R. E. Baker, *ibid.* **73**, 2527 (2011).
- [24] R. A. Fisher, *Ann. Eugenics* **7**, 355 (1937).
- [25] V. Tikhomirov, in *Selected Works of A. N. Kolmogorov*, edited by V. Tikhomirov, Mathematical Applications (Soviet Series) Vol. 25 (Springer, New York, 1991), pp. 242–270.
- [26] J. Hsia, W. J. Holtz, D. C. Huang, M. Arcak, and M. M. Maharbiz, *PLoS Comput. Biol.* **8**, e1002331 (2012); H. Miyazako, Y. Hori, and S. Hara, in *Proceedings of the 52nd IEEE Conference on Decision and Control, Firenze, Italy 2013* (IEEE, New York, 2013), p. 2671.
- [27] V. Klika, R. E. Baker, D. Headon, and E. A. Gaffney, *Bull. Math. Biol.* **74**, 935 (2012).
- [28] A. Marciniak-Czochra, G. Karch, and K. Suzuki, *J. Math. Biol.* **74**, 583 (2017).
- [29] J. Petit, T. Carletti, M. Asllani, and D. Fanelli, *Europhys. Lett.* **111**, 58002 (2015).
- [30] P. Ghosh, S. Sen, and D. S. Ray, *Phys. Rev. E* **81**, 026205 (2010).
- [31] G. E. Hutchinson, *Ann. NY Acad. Sci.* **50**, 221 (1948).
- [32] H. L. Smith, *Math. Bio.* **113**, 1 (1993).
- [33] D. Ewing, C. Cobbold, B. Purse, M. Nunn, and S. White, *J. Theor. Bio.* **400**, 65 (2016).
- [34] A. Otto and G. Radons, Transformations from variable delays to constant delays with applications in engineering and biology, in *Time Delay Systems: Theory, Numerics, Applications, and Experiments*, edited by T. Insperger, T. Earsal, and G. Orosz (Springer, Berlin, 2017), pp. 169–183.
- [35] L. Champine, *Appl. Num. Math.* **52**, 113 (2005).
- [36] A. Pikovsky, M. Rosenblum, and J. Kurths, *Synchronization: A Universal Concept in Nonlinear Sciences* (Cambridge University Press, Cambridge, 2003).
- [37] L. M. Pecora and T. L. Carroll, *Phys. Rev. Lett.* **80**, 2109 (1998).
- [38] W. Michiels, V. V. Assche, and S.-I. Niculescu, *IEEE Trans. Autom. Control* **50**, 493 (2005).
- [39] W. Michiels and S.-I. Niculescu, *Stability and Stabilization of Time-Delay Systems, An Eigenvalue Based Approach* (SIAM Publications, Philadelphia, PA, 2007).
- [40] T. Insperger and G. Stépán, *Semi-Discretization for Time-Delay Systems: Stability and Engineering Applications* (Springer, Berlin, 2011).
- [41] A. Wolf, J. B. Swift, H. L. Swinney, and J. A. Vastano, *Physica D* **16**, 285 (1985); L. Dieci and E. S. V. Vleck, *Appl. Numer. Math.* **17**, 275 (1995).
- [42] R. Corless, D. Jeffrey, and D. Knuth (eds.), *A Sequence of Series for the Lambert Function*, ISSAC (ACM, Maui, HI, 1997); J. Lambert, *Acta Helveticae physico-mathematico-anatomico-botanico-medica* **3**, 128 (1758).
- [43] C. A. J. Fletcher, *Computational Techniques for Fluid Dynamics* (Springer, Berlin, 1989), Vol. I.
- [44] M. Farkas, *Periodic Motions* (Springer, New York, 1994).
- [45] A. Otto, G. Kehl, M. Mayer, and G. Radons, *Adv. Mater. Res.* **223**, 600 (2011); A. Otto and G. Radons, *CIRP J. Manuf. Sci. Technol.* **6**, 102 (2013).
- [46] A. Amann, E. Schöll, and W. Just, *Physica A* **373**, 191 (2007).
- [47] A. Otto, Frequency domain methods for the analysis of time delay systems, Ph.D. thesis, TU Chemnitz, 2016.
- [48] M. Born and V. A. Fock, *Z. Phys. A* **51**, 165 (1928).
- [49] M. Bestehorn and P. Colinet, *Physica D* **145**, 84 (2000).
- [50] E. Ott, *Chaos in Dynamical Systems* (Cambridge University Press, New York, 2002).
- [51] L. Barreira and C. Valls, *Stability of Nonautonomous Differential Equations* (Springer, New York, 2008).
- [52] V. Petrov, Q. Ouyang, and H. L. Swinney, *Nature (London)* **388**, 655 (1997).
- [53] L. Jaurigue, E. Schöll, and K. Lüdge, *Phys. Rev. Lett.* **117**, 154101 (2016).